Optics Letters

Sub-second infrared broadband-laser single-shot phase–amplitude polarimetry of thin films

Andreas Furchner,* Christoph Kratz, and Karsten Hinrichs

Leibniz-Institut für Analytische Wissenschaften—ISAS—e. V., Schwarzschildstraße 8, 12489 Berlin, Germany
**Corresponding author: andreas.furchner@isas.de*

Received 10 July 2019; revised 27 July 2019; accepted 29 July 2019; posted 30 July 2019 (Doc. ID 372280); published 29 August 2019

We report on the first, to the best of our knowledge, sub-second, sub-mm^2 infrared (IR) spectroscopic measurements of thin organic films employing a laser-based phase–amplitude polarimeter in reflection geometry. The polarimeter uses a broadband mid-IR quantum cascade laser tunable between 1318 cm^{-1} and 1765 cm^{-1}, as well as a single-shot beam division scheme for simultaneous single-pulse phase and amplitude measurements. The instrument achieves 120 µm spatial and <0.5 cm^{-1} spectral resolution, while providing unrivaled performance in terms of acquisition times. Spectral measurements within 100 ms and single-wavelength tracking at 16 µs are now possible. Investigating the vibrational properties accessible in the mid-IR, the polarimeter was applied for monitoring changes in molecular interactions of a 150 nm thin myristic acid film during its thermal phase transition around 55°C.

https://doi.org/10.1364/OL.44.004387

Polarimetry, often termed ellipsometry, is a well-established, reference-free, thin-film-sensitive technique that measures the changes in polarization state of light upon interaction with a sample [1–4]. This change, expressed as amplitude ratio tan Ψ and phase difference Δ, is related to the sample's geometrical and optical properties, rendering the method sensitive to both structural information and complex refractive indices without the need for Kramers–Kronig analysis. Polarimetry of thin films in the IR spectral range is of wide interest for a plethora of scientific and technological applications, as it gives access to material-specific vibrational bands that provide insights into chemical composition, anisotropy, and molecular orientation, but also surface morphology, homogeneity, hydration, and molecular interactions [4].

Until recently, the sensitivity of conventional laboratory-based (Fourier-transform, FT-IR) ellipsometers was limited by their thermal light sources, which exhibit low brilliance, i.e., low photon flux per solid angle and optical bandwidth, resulting in long integration times to achieve sufficient signal-to-noise ratios (SNRs) at only mm^2 lateral resolutions. Synchrotron ellipsometry [5–8] played an important role regarding sub-mm^2 measurements. With the inexorable developments in IR laser technology, quantum cascade lasers (QCLs) now constitute powerful laboratory radiation sources that provide high coherence, broad bandwidth, and high brilliance, and thus potentially profound improvements of SNR and measurement speed at diffraction-limited spatial resolutions.

The first instruments using IR QCLs addressed vibrational circular dichroism [9], absorbance imaging of tissue micro arrays [10], multi-wavelengths scatterometry of nanostructured materials [11], ellipsometric mapping of structured surfaces, and interactions in organic thin films [12], as well as transmission ellipsometry of anisotropic thick polymer films [13].

Still lacking, however, is an IR polarimeter that enables sensitive studies of processes in organic thin films at sub-s temporal, sub-mm^2 spatial, and sub-1 cm^{-1} spectral resolution. In an earlier design phase [12], we successfully coupled a QCL with an ellipsometer that used two parallel polarization-detection channels for single-shot spectral tan Ψ measurements without rotating polarizers. With time resolutions of 60 ms per wavelength, this device illustrated the prospects for fast mapping of heterogeneous thin films, albeit at only mm^2 spatial resolution.

We have improved the established concept and now present a new polarimeter that is based on a four-channel detection scheme for simultaneous single-shot phase–amplitude measurements of individual laser pulses. The instrument unleashes the full potential of IR laser polarimetry, establishing measurements with unprecedented time resolution of <200 µs for the analysis of small sample areas of 280 µm × 120 µm. The implementation of a pulsed QCL in a division-of-wavefront [14] configuration allows for thin-film-sensitive and spectrally highly resolved (<0.5 cm^{-1}) measurements of the ellipsometric angles Ψ and Δ.

In comparison to classical FT-IR ellipsometry, the novel instrument performs simultaneous measurements of four different polarization states, and thereby unlocks a time range from a few 10 µs to a few seconds for sensitive polarimetry of non-cyclic processes, such as adsorption kinetics or phase transitions. Beyond single-wavelength measurements at maximum time resolution, sub-decisecond broadband spectral measurements for detailed vibrational band analyses now become possible.

In an upcoming article, we will cover the device's hyperspectral imaging capabilities for the mapping of chemical and

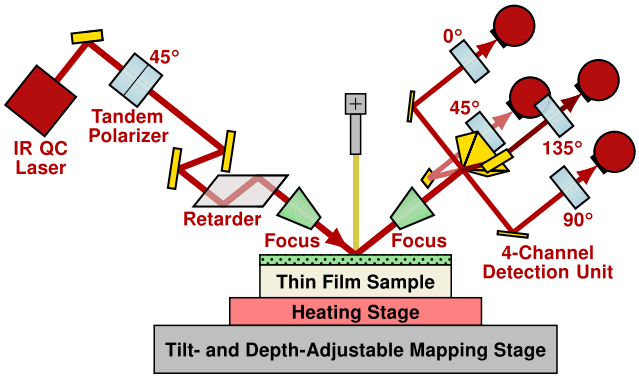

Fig. 1. Schematic of the four-channel single-shot IR laser ellipsometer.

structural film properties. Here, we will focus on time-resolved single-shot phase–amplitude measurements, applying the instrument to investigations of the thermal phase transition of thin films of myristic acid (MA), a fatty acid with promising applications in biomedicine [15,16] and phase-change materials for energy storage [17,18].

The polarimeter (Sentech Instruments GmbH), schematically depicted in reflection geometry in Fig. 1, is built around a movable (50 mm × 50 mm) tilt- and height-adjustable sample mapping stage with an autocollimation unit, which enables sample alignment with respect to the instrument's input and output arms. The input arm consists of an external-cavity QCL (MIRcat 2100, Daylight Solutions), followed by a tandem pair of KRS-5 wire-grid polarizers (0.25 μm wire spacing, Specac Ltd.) oriented at 45°, and an optional retarder [19] for sensitive phase measurements near $\cos\Delta \approx \pm 1$. The polarizer is slightly tilted to avoid backreflections into the QCL cavity. The output arm comprises a fully angle- and position-adjustable four-channel detection unit, in which the output beam is split into four subbeams using a four-faceted gold pyramid. Gold-coated off-axis parabolic mirrors (25 mm focal length) focus the subbeams through KRS-5 wire-grid polarizers onto four photovoltaic InAsSb detectors (P13894-211, Hamamatsu).

With the four polarizers in the detection channels fixed at orientations of 0°, 90°, 45°, and 135°, the polarimeter is basically an IR ellipsometer after Röseler's four-intensity scheme [20] to obtain the ellipsometric ratio

$$\varrho = \tan\Psi \cdot e^{i\Delta} = \frac{r_p}{r_s} \tag{1}$$

in a synchronized single-shot intensity measurement from

$$\cos 2\Psi = \frac{I_{90°} - I_{0°}}{I_{90°} + I_{0°}}, \qquad \sin 2\Psi \cos\Delta = \frac{I_{45°} - I_{135°}}{I_{45°} + I_{135°}}. \tag{2}$$

The ellipsometric parameters $\tan\Psi$ and Δ are the amplitude ratio and phase difference between the complex reflection coefficients parallel (p) and perpendicular (s) to the plane of incidence. A known reference sample in reflection, or a measurement of air in transmission, is used to calibrate the beam division at the gold pyramid.

The four detectors are read out via gated integrators (custom-built boxcar electronics) that average the signals over each individual laser pulse. This four-channel scheme thus enables single-shot Ψ and Δ measurements at the level of the laser repetition rate. Time resolutions down to 16 μs (61 kHz) are currently possible in single-wavelength mode. For spectral measurements, the emitting wavelength of this particular QCL is tunable between 1318 cm^{-1} and 1764 cm^{-1} with sweep speeds up to ≈1500 cm^{-1}/s. It typically takes merely a few 100 ms (< 200 μs per wavelength) to collect a whole spectrum with sufficient SNR. Spectral ranges smaller than 100 cm^{-1} can be measured even faster than 100 ms.

The QCL beam has a spectral linewidth of 0.4 cm^{-1} with wavelength stability and repeatability ≤ 0.1 cm^{-1}. Full-range spectra can be recorded at a spectral resolution of 0.2 cm^{-1}, which is well below the resolution of many commercial, non-laser-based devices.

The average laser power at the sample stage is wavelength dependent but less than 10 mW. For measurements of sensitive samples, the laser's duty cycle and/or current can be reduced.

The laser operates in the TEM_{00} mode, emitting a beam with a waist of about 2.5 mm. Different sets of CaF_2 micro-focus lenses (Plano-Convex, uncoated, Thorlabs) can be mounted before and after the sample to reduce the probed spot on the sample to as small an area as 280 × 120 μm^2 (at 65° incidence angle). For the experiments presented here, lenses with a focal length of 91.7 mm were used, yielding a spot of about 590 μm × 250 μm.

Samples were placed on a *Linksys 32* heating stage (Linkam Scientific Instruments Ltd.) for temperature-related experiments.

To demonstrate the measurement capabilities of the instrument, we investigated thin organic films of MA on gold substrates. For this purpose, MA films were prepared by dissolving MA (Sigma Grade ≥ 99%, Sigma Aldrich) in acetone (Emsure ACS, ISO, Reag. Ph. Eur., Merck KGaA) with a concentration of 15 mg/ml, and then applying 20 μl drops of the solution to gold-coated glass microscopy slides (SSens B.V.). After evaporation of the acetone at room-temperature, the films were left to equilibrate for a week under ambient conditions.

Both amplitude ($\tan\Psi$) and phase ($\cos\Delta$) spectra of a 150 nm thick MA layer were acquired over the full accessible QCL range (Fig. 2), providing an overview of MA's vibrational features. Similar to k and n of thin films, the vibrational band shapes are absorption-band-like in $\tan\Psi$ and derivative-like $\cos\Delta$. The prominent band around 1705 cm^{-1} is associated with the stretching mode, $\nu(C{=}O)$, of the fatty acid's carboxyl groups. The bands between 1318 cm^{-1} and 1500 cm^{-1} are related mainly to modes of MA's saturated aliphatic chains.

The spectra were recorded at 0.2 cm^{-1} spectral resolution and smoothed with a 1 cm^{-1} moving-average filter. To judge how SNR and measurement time compare with those of other, non-laser-based devices, we measured the same MA film with one of our home-built, high-sensitivity, high-throughput-optimized laboratory FT-IR ellipsometers. Corresponding data are also shown in Fig. 2. Here, a spectral resolution of 1.0 cm^{-1} was used. To achieve a comparable measurement area on the sample, the FT-IR spectrometer's Jacquinot aperture was set to 0.25 mm for the smallest feasible spot size of about 1.4 mm × 0.6 mm. Thirty-two FT-IR scans were accumulated at each polarizer setting.

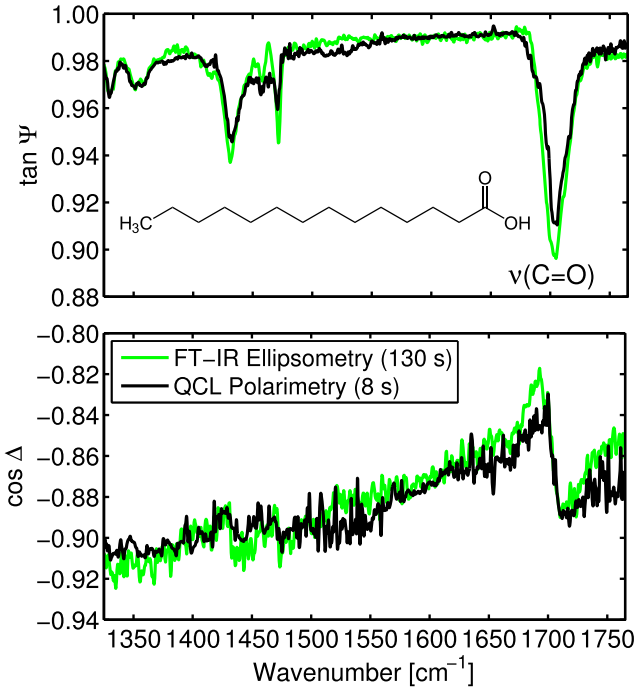

Fig. 2. Overview of polarimetric amplitude (tan Ψ) and phase (cos Δ) spectra of a 150 nm MA film compared with data from high-sensitivity FT-IR ellipsometry. The FT-IR set-up needed to be purged with dried air (r.H. ≪ 0.1%), whereas the QCL single-shot set-up was operated under ambient conditions (r.H. > 20%). The inset shows MA's chemical structure.

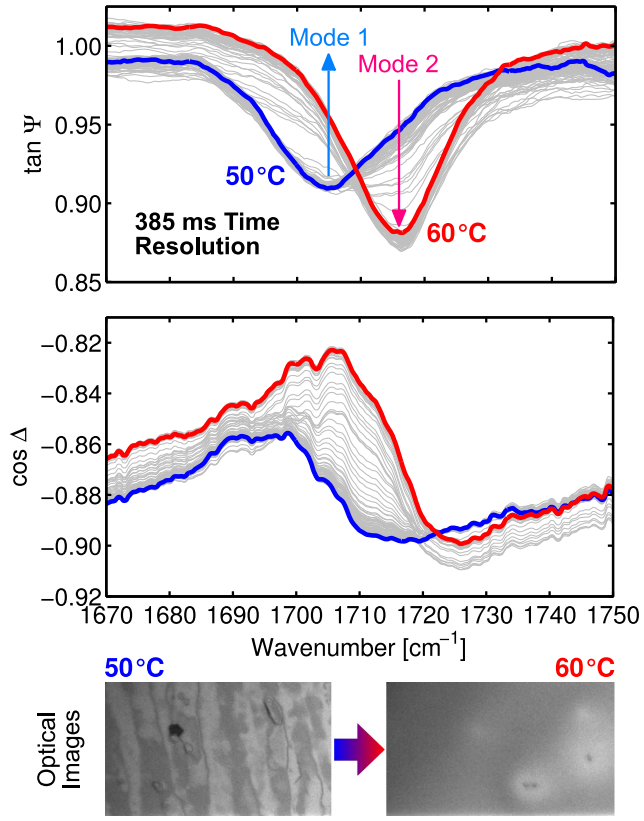

Fig. 3. Top: Time-resolved polarimetric spectra of the MA film's ν(C=O) band during heating above MA's phase-transition temperature. Data were recorded in 0.056 cm^{-1} steps and smoothed with a 4 cm^{-1} moving-average filter. Bottom: optical images (140 μm × 80 μm within the measured area) of the film's crystallized state below and liquid-like state above the transition.

For the above parameters, the noise levels of both instruments are very similar. However, with 8 s (20 accumulated scans), the QCL single-shot polarimeter is about 16× faster than the FT-IR ellipsometer (130 s), or about 100× faster considering the 6× smaller spot size. This advancement is due, in large part, to the superior brilliance of the QCL, but also because the polarimeter works in a single-shot configuration without any moving parts during data acquisition (except for the rotating QCL grating for spectral sweeps).

Note that commercial IR ellipsometers are usually equipped with pyroelectric detectors, which are several orders of magnitude less sensitive than the photovoltaic HgCaTe detector used to obtain the presented FT-IR ellipsometry data. For measurements with sub-mm^2 spot sizes and/or high spectral resolutions ($\leq$ 1 cm^{-1}), our novel QCL-based polarimeter therefore significantly outperformes conventional devices, improving measurement time and/or SNR by orders of magnitude.

In the following, we exploit the polarimeter's unprecedented time resolution for studying the thermal behavior of MA thin films. We focus on the temperature-sensitive ν(C=O) mode, which is highly susceptive to changes in intermolecular interactions and chemical environments. Restricting the wavelength range to a few 10 cm^{-1} also has the benefit of yielding a significantly higher SNR at the same spectral resolution.

Starting at room temperature, the MA film was heated to above its critical temperature of $T_c \approx 55$°C at a rate of 5°C per min. Figure 3 shows corresponding tan Ψ and cos Δ spectra between 50°C and 60°C measured with a time resolution of 385 ms (or 190 μs per wavelength). The phase transition is monitored via changes in the ν(C=O) band composition. Below the transition, the band is described mainly by one component at 1705 cm^{-1}, termed mode 1. Upon heating, a second component at 1716 cm^{-1}, mode 2, gains intensity while mode 1 diminishes. The ν(C=O) band becomes unimodal above T_c, containing only mode 2.

The temporal evolution of the two ν(C=O) components was fitted using two Voigt oscillators [21]. As shown in Fig. 4, their amplitudes exhibit gradual changes between 0 s and 30 s approaching T_c, followed by a sharp transition occurring between 32 s and 37 s. The transition shapes are reminiscent of the thermoresponsive behavior of materials such as PNIPAAm brushes [22], whose temperature-induced phase transition in water is governed by changes in amide–amide and amide–water hydrogen-bond patterns [21,23].

We propose that the observed changes in the MA film's ν(C=O) band composition are also associated with hydrogen bonding, i.e., with hydrogen-bond formation below MA's melting point accompanied by molecular reorientation during film crystallization, and with breaking of hydrogen bonds above T_c where the fatty-acid film exists in a liquid-like state. Above the critical temperature, the chains exhibit high thermal mobility, rendering close-range molecular interactions such as hydrogen bonding unlikely to occur. This state is associated with mode 2 at 1716 cm^{-1}. Below the critical temperature, the film is

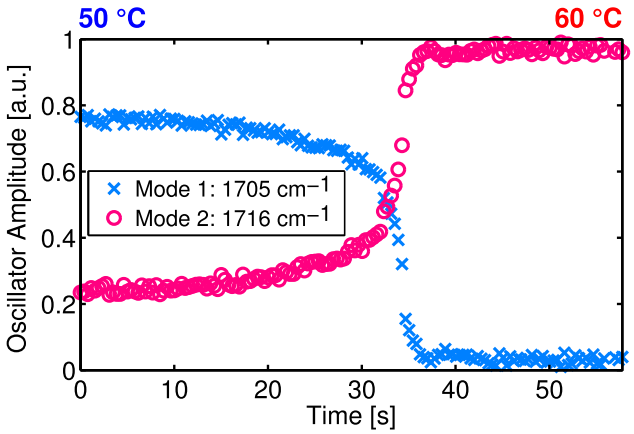

Fig. 4. Fitted time-resolved evolution of the two ν(C=O) band components with heating temperature. Slightly higher than expected, the apparent sharp phase-transition temperature is observed at about 55.9°C due to the delayed heat transfer through the thick glass substrate.

crystallized, and the thermal energy is small enough for MA's carboxyl groups to form dimers and other hydrogen-bond arrangements between adjacent C=O and HO groups [24]. Hydrogen bonding leads to a pronounced red shift of the associated ν(C=O) oscillations, i.e., to mode 1 at 1705 cm^{-1}.

Hydrogen-bond formation seems to coincide with reorientation effects of the fatty-acid chains as the film crystallizes, which we also observed right after film preparation. Both modes are found in the freshly prepared state, but mode 1 disappears almost completely after a one-week equilibration. According to Fig. 4, about 80% of carboxyl groups are involved in hydrogen-bond interactions in the crystallized state.

These first results already highlight the vast potential of sub-second IR laser polarimetry for detailed time-resolved studies of the properties of thin organic films.

We are currently working on coupling microfluidic flow cells to the instrument in order to investigate solid–liquid interfaces with unparalleled spatial and temporal resolution. Applications are measurements of processes and molecular interactions in electrochemistry, catalysis, and bioanalytics, e.g., reaction processes at surfaces, stimuli-responsive interactions and phase transitions of thin polymer films, diffusion processes in membranes, and the investigation of protein signal transduction, protein kinetics, as well as studies of macromolecular aggregation. For faster, sub-ms processes, we will operate the device in single-wavelength mode to monitor vibrational changes at up to 16 μs temporal resolution. Such measurement speeds will facilitate the monitoring and quantification of, e.g., adsorption kinetics and molecular reorientation effects at low surface coverage.

Various technical upgrades, such as water cooling of the laser, could lead to further significant improvements in stability and SNR. By purging the instrument with dried air, for example, we expect a SNR increase of up to 50% in the vicinity of the water-vapor absorption bands.

Currently, the polarimeter's detection channels can measure R_p, R_s, and the corresponding phase difference. However, the four channels could, in principle, be modified to detect arbitrary polarization states, which is of interest for direct measurements of, e.g., circular dichroism and other specific polarimetric properties associated with the sample's Mueller matrix.

Funding. Europäischer Fonds für regionale Entwicklung (EFRE) (1.8/13); Ministerium für Innovation, Wissenschaft und Forschung des Landes Nordrhein-Westfalen; Regierende Bürgermeister von Berlin—Senatskanzlei Wissenschaft und Forschung; Bundesministerium für Bildung und Forschung.

Acknowledgment. The instrument was designed and set up in close collaboration with Sentech Instruments GmbH. We thank Uwe Richter, Johanna Reck, Konstantin Schreiter, Frank Günther, and Mike Hofmann for their support. We also thank Matthias Godejohann (MG Optical Solutions GmbH) who provided valuable information on laser and boxcar electronics, Klaus-Jochen Eichhorn (IPF Dresden) and Jörg Rappich (HZB in Berlin) for fruitful discussions, and Özgür Savas (ISAS Berlin) for technical assistance.

REFERENCES

1. H. G. Tompkins and E. A. Irene, *Handbook of Ellipsometry* (William Andrew, 2005).
2. H. Fujiwara, *Spectroscopic Ellipsometry: Principles and Applications* (Wiley, 2007).
3. M. Losurdo and K. Hingerl, *Ellipsometry at the Nanoscale* (Springer, 2013).
4. K. Hinrichs and K.-J. Eichhorn, *Ellipsometry of Functional Organic Surfaces and Films* (Springer, 2018).
5. M. Gensch, K. Hinrichs, A. Röseler, E.-H. Korte, and U. Schade, Analytical and Bioanalytical Chemistry **376**, 626 (2003).
6. C. Bernhard, J. Humlíček, and B. Keimer, Thin Solid Films **455–456**, 143 (2004).
7. K. Roodenko, Y. Mikhaylova, L. Ionov, M. Gensch, M. Stamm, S. Minko, U. Schade, K.-J. Eichhorn, N. Esser, and K. Hinrichs, Appl. Phys. Lett. **92**, 103102 (2008).
8. T. Stanislavchuk, T. Kang, P. Rogers, C. Standard, R. Basistyy, A. Kotelyanskii, G. Nita, T. Zhou, G. Carr, M. Kotelyanskii, and A. Sirenko, Rev. Sci. Instrum. **84**, 023901 (2013).
9. S. Lüdeke, M. Pfeifer, and P. Fischer, J. Am. Chem. Soc. **133**, 5704 (2011).
10. P. Bassan, M. J. Weida, J. Rowlette, and P. Gardner, Analyst **139**, 3856 (2014).
11. J. C. Vap, S. E. Nauyoks, M. R. Benson, and M. A. Marciniak, Rev. Sci. Instrum. **88**, 103104 (2017).
12. A. Furchner, C. Kratz, D. Gkogkou, H. Ketelsen, and K. Hinrichs, Appl. Surf. Sci. **421**, 440 (2017).
13. A. Ebner, R. Zimmerleiter, C. Cobet, K. Hingerl, M. Brandstetter, and J. Kilgus, Opt. Lett. **44**, 3426 (2019).
14. R. M. A. Azzam, Thin Solid Films **234**, 371 (1993).
15. I. Matai and P. Gopinath, RSC Adv. **6**, 24808 (2016).
16. J. M. Silva, S. Akkache, A. C. Araújo, Y. Masmoudi, R. L. Reis, E. Badens, and A. R. C. Duarte, Mater. Sci. Eng. C **99**, 599 (2019).
17. K. Pielichowska and K. Pielichowski, Prog. Mater. Sci. **65**, 67 (2014).
18. S. Y. Kee, Y. Munusamy, K. S. Ong, H. Simon, C. Metselaar, S. Y. Chee, and K. C. Lai, Materials **10**, 873 (2017).
19. A. Furchner, C. Walder, M. Zellmeier, J. Rappich, and K. Hinrichs, Appl. Opt. **57**, 7895 (2018).
20. A. Röseler and E.-H. Korte, *Handbook of Vibrational Spectroscopy*, J. M. Chalmers and P. R. Griffiths, eds. (Wiley, 2006).
21. A. Furchner, A. Kroning, S. Rauch, P. Uhlmann, K.-J. Eichhorn, and K. Hinrichs, Anal. Chem. **89**, 3240 (2017).
22. E. Bittrich, S. Burkert, M. Müller, K.-J. Eichhorn, M. Stamm, and P. Uhlmann, Langmuir **28**, 3439 (2012).
23. Y. Maeda, T. Higuchi, and I. Ikeda, Langmuir **16**, 7503 (2000).
24. L. F. L. da Silva, T. Andrade-Filho, P. T. C. Freire, J. M. Filho, J. G. da Silva Filho, G. D. Saraiva, S. G. C. Moreira, and F. F. de Sousa, J. Phys. Chem. A **121**, 4830 (2017).